

Supplementary Material

Kinesin walks the line: single motors observed by atomic force microscopy

Iwan A. T. Schaap, Carolina Carrasco, Pedro J. de Pablo, Christoph F. Schmidt

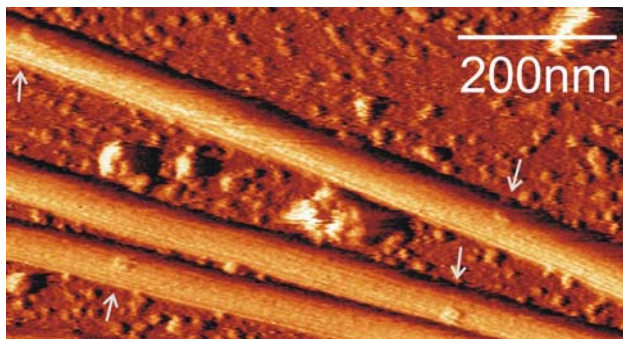


Figure S1. Overview scan of multiple MTs with bound kinesin motors.

The image was processed with a derivative filter. Three MTs are shown, each with a height of 25 nm. On top the protofilaments are visible as lines parallel to the MT axis. Kinesin motors in the presence of AMP-PNP are visible as blobs (arrows) bound to the MT. At this resolution the individual heads are not clearly distinguishable.

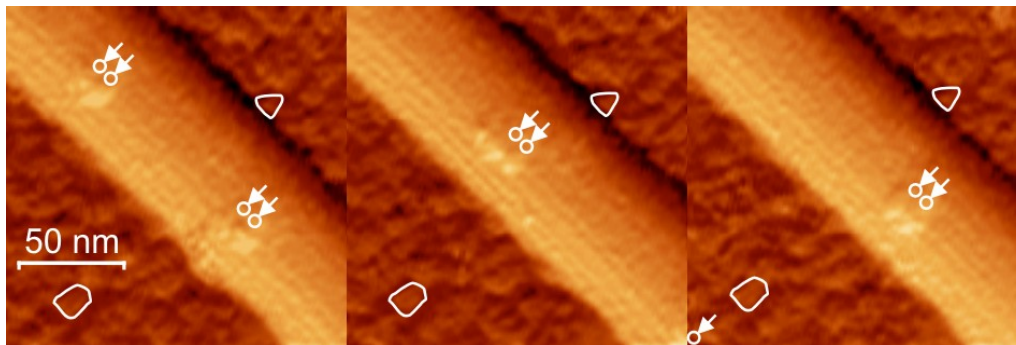


Figure S2. Top-view rendering of Figs 3a-c.

Left: Two kinesin dimers, the heads are indicated with arrows. Middle: Both motors have proceeded, from the leading kinesin only the last head is still visible (indicated by the single arrow). Right: The second kinesin has proceeded further.

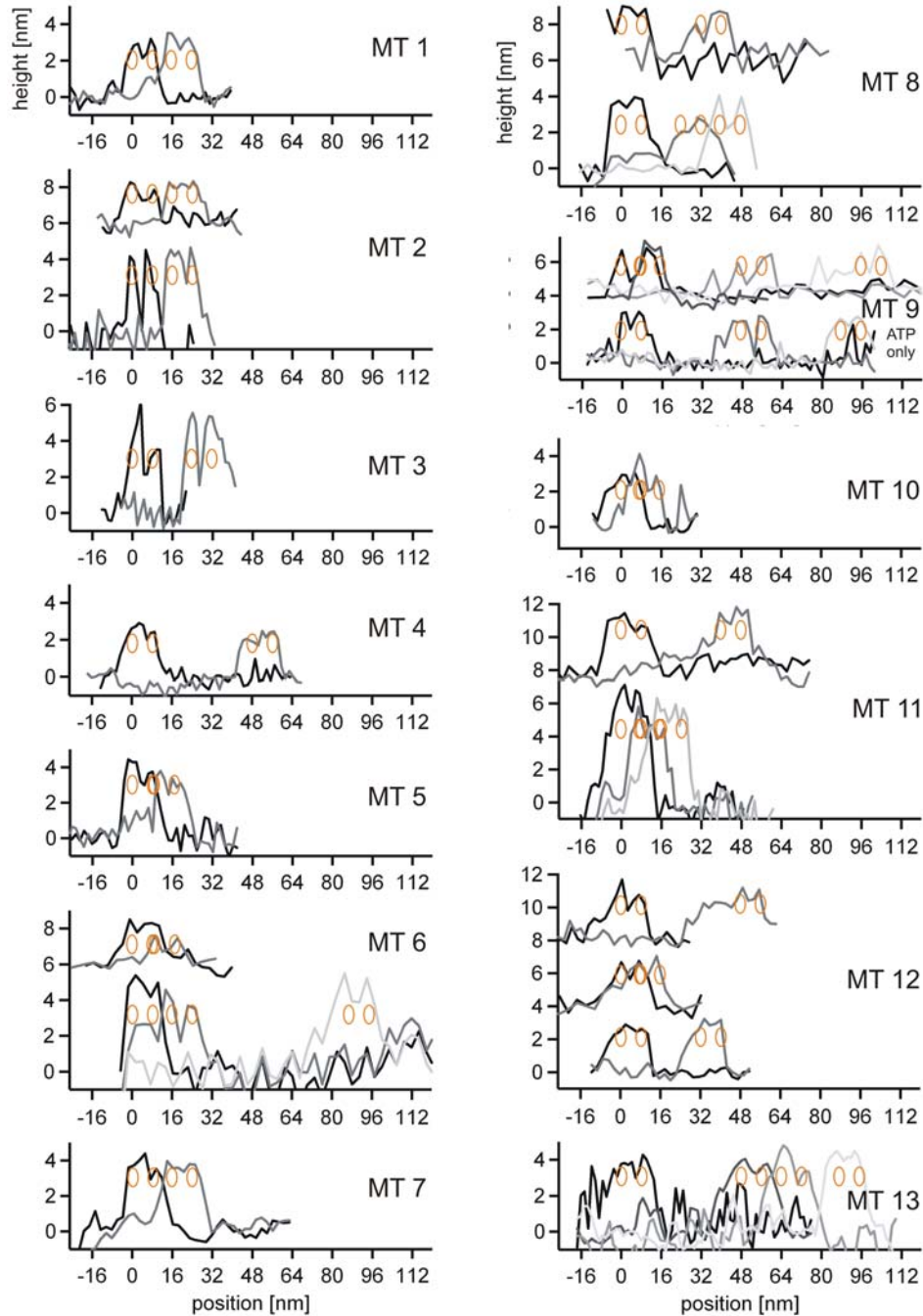


Figure S3. Topographical profiles along the MT axis of all kinesin dimers recorded in motion on 13 different MTs.

The black profile in each graph stems from the respective first frame, the dark grey from the second, the lighter grey from the third, etc. As kinesin heads we identified those features in the profiles that showed a height of at least 2 nm and a length of at least 5 nm. When multiple events took place on the same MT, these are plotted in one graph. The observed directionality on the same MT was always the same. The orange circles, plotted on an 8 nm raster, represent the presumed positions of the kinesin heads. For most experiments AMP-PNP was washed out by rinsing the sample 5 times with buffer containing 0.5-2 μ M ATP. Only the two events that were recorded on MT 9 were performed without the pre-incubation step with AMP-PNP.

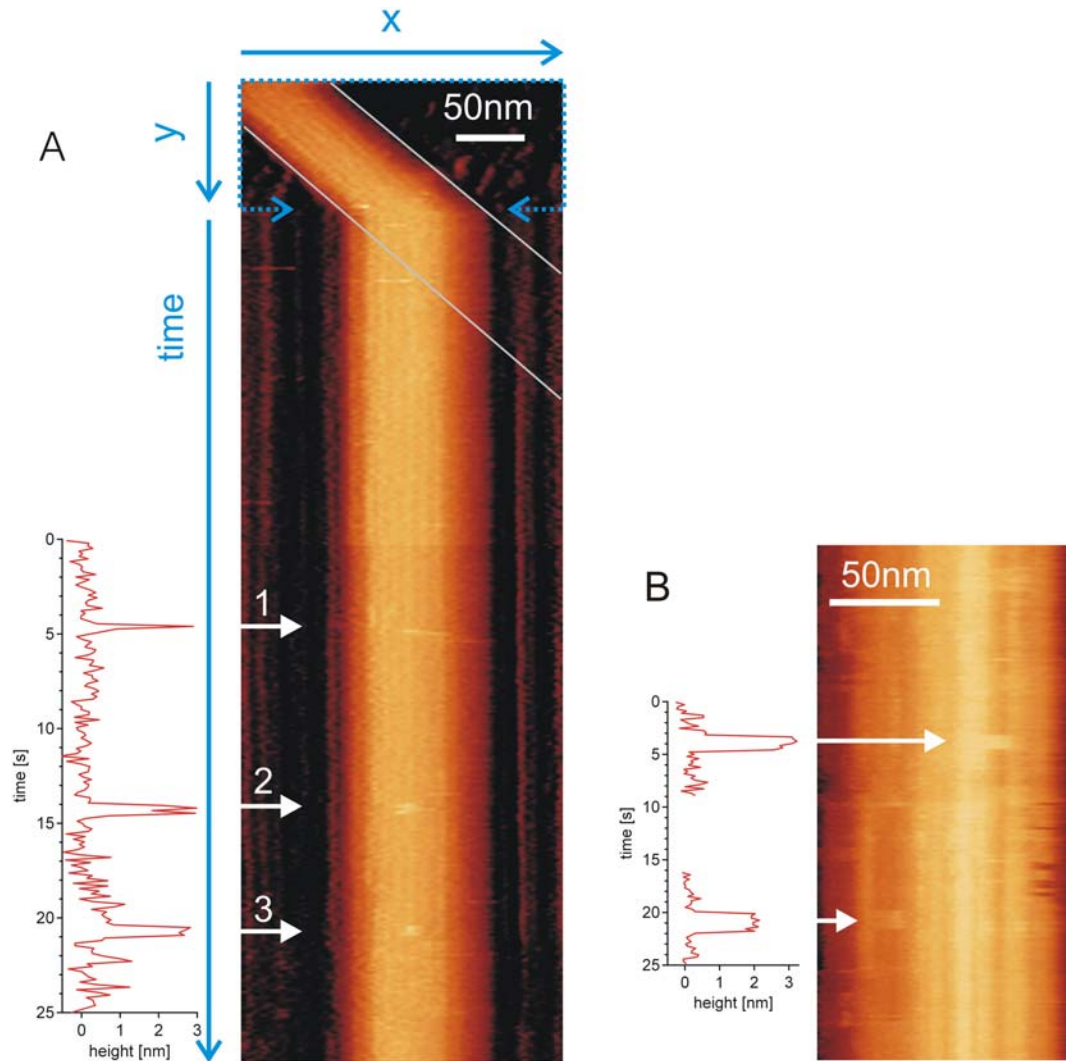


Figure S4. Line-scan. a. The top part of the image, enclosed by the blue dotted line, shows the diagonal oriented MT, scanned with 128 pixels per scan-line. After having scanned 100 nm in y-direction, the y-scanning was switched off, such that the same line across the MT was scanned again and again. The resulting x vs. time scan is shown in the lower part of the image. The line frequency was 7.3 Hz and the x-scan direction was scanned in only one direction (trace). During the line scan sudden increases in height are visible that are likely to be caused by kinesin motors passing by. The height profile (plotted in red) that was taken through the center of the x vs. time scan shows that first event is very short lived and may be a motor that was wiped off the MT due to the scanning action of the tip. The second and third events lasted each for about 1 second and show an increase in height of about 3 nm, consistent the height shown in Fig. 4b.

b. Line-scan from a different experiment. The MT was scanned with 128 pixels per scan-line and with a line frequency of 4.9 Hz. The height profile shows two events with a height of 2-3 nm and a duration of 2 s.

Statistical analysis of kinesin motility events

We observed 20 isolated kinesin motors that appeared to proceed along a single protofilament in consecutive frames of recorded movies. We counted 14 one-step, 4 two-step, and 2 three-step events. For an additional 6 kinesin motors we observed what appeared to be a lateral displacement in consecutive frames, from one protofilament to a neighboring one.

To prove the point that motors mostly track along single protofilaments, we need to control against the possibility that the observed events, instead of reflecting processive motor movement of one motor, resulted from random unbinding and re-binding of (different) kinesin motors or from the walking out of the field of view of one motor and walking into the field of view of another motor in positions that make it look like processive motion of a single motor. We thus used all our recordings to estimate an upper bound on the probability that one motor unbound or walked away from a particular position in one frame and another motor ended up in the next frame anywhere on the same protofilament by binding or walking into the field of view, for two or more consecutive frames. We determined the mean rates of motor appearance on a previously unoccupied position and disappearance from a previously occupied position by comparing consecutive frames. We deliberately include the cases that we actually think are events of the same motor moving forward to obtain the worst-case scenario. Using those rates, we estimated the number of “false” 1- 2- and 3-step events expected and then estimated the probability to obtain the actually observed number of the respective events in the two-independent-motors scenario.

Motors can appear in a video frame either by attaching from solution or by walking into the scanned image area during the time it takes to record one frame, and, likewise, they can disappear either by detaching or by walking away from the previously occupied position. We obtained average rates of appearance in a previously unoccupied position and of disappearance from a previously occupied position at the motor concentration we used by counting the number of kinesins appearing in a previously unoccupied position from one frame to the next, and the number of kinesins disappearing from a previously occupied position from one frame to the next. A subtle issue concerns the possibility that a motor binds and then within the same frame time unbinds again without being seen on the image. Such cases lead to an underestimate of the rate of motor binding. To obtain a worst-case estimate we assume that a motor is only detected when it is present at the very end of the frame time and that it has a whole frame time to unbind before being seen. In reality a motor can still be detected with a finite probability even when the rate of disappearance is close to 1/frame/motor, because it can bind directly before the tips reaches its location and therefore have no chance to unbind. The observed appearance rate λ_{app}^{obs} can thus be used to estimate the actual appearance rate λ_{app} using:

$$\lambda_{app}^{obs} \approx \lambda_{app} (1 - \lambda_{dis}) \quad \text{Eq. S1}$$

To get the average appearance rate per frame λ_{app}^{obs} , we divide the counted appearance events by the total number of frames recorded minus the number of movies recorded (441-23 = 418) since at least two frames are required to see a motor appear, i.e. we cannot count the first frame of each movie. See table S1 for all observation statistics.

To estimate the disappearance rate, we again assume the worst case and call every event when a motor leaves a particular binding site between one frame and the next an unbinding

event, irrespective of the possibility that the motor might have staid bound, but moved along. Here we neglect the very unlikely events where one motor unbinds and another motor rebinds in the exact same position within the frame time. To get the average disappearance rate per frame per motor $\lambda_{dis}^{obs} \approx \lambda_{dis}$, we divide the number of disappearance events (103) by the number of frames with motors present weighted by the average number of motors present (418*2.41=1006).

Table S1. Observation statistics. From all experiments we performed in the presence of ATP.

MTs imaged	13
Movies recorded	23
Frames recorded	441
Kinesin motors imaged	1061
Average number of motors per frame	2.41
Number of motors appearing	63
Average rate of motor binding, per frame (λ_{app})	0.168
Number of motors disappearing	103
Average rate of motor unbinding, per frame, per motor (λ_{dis})	0.102

Frames were 156 x 156 nm in size and typically showed diagonally oriented microtubules with a length of about 180 nm. Typically we could only resolve fine structure and bound motors on the top three protofilaments. With an average motor velocity on the order of several nm/s and frame-acquisition times of around 30 s, motors can perform several 8 nm steps from frame to frame. We thus counted as potential motility events, all those during which a motor was repeatedly imaged on the same protofilament, but away from the first appearance site. For multiple-step events, movement had to be consistently in the same direction.

To estimate the expected number of “false” steps from two-independent-motor events, given the average rates we determined, as described above, we now assume that appearance and disappearance of motors are independent of each other and follow Poisson statistics. The probability for a “false” 1-step event P_1 is thus the probability for disappearance multiplied with the probability of appearance on the same protofilament between two frames (Eq. S2). The probability for a “false” 2-step event P_2 will be P_1 multiplied by again the probability for disappearance and the probability of appearance, but now on a (roughly) half protofilament in the right direction, and accordingly for P_3 (Eqs. S3 & 4):

$$P_1 = \lambda_{dis} \frac{\lambda_{app}}{3} e^{-\left(\lambda_{dis} + \frac{\lambda_{app}}{3}\right)} \quad \text{Eq. S2}$$

$$P_2 = \lambda_{dis} \frac{\lambda_{app}}{3} e^{-\left(\lambda_{dis} + \frac{\lambda_{app}}{3}\right)} \lambda_{dis} \frac{\lambda_{app}}{6} e^{-\left(\lambda_{dis} + \frac{\lambda_{app}}{6}\right)} \quad \text{Eq. S3}$$

$$P_3 = \lambda_{dis} \frac{\lambda_{app}}{3} e^{-\left(\lambda_{dis} + \frac{\lambda_{app}}{3}\right)} \left(\lambda_{dis} \frac{\lambda_{app}}{6} e^{-\left(\lambda_{dis} + \frac{\lambda_{app}}{6}\right)} \right)^2 \quad \text{Eq. S4}$$

The factor $1/3$ multiplying λ_{app} takes into account that the appearance has to occur on the proper one of three visible protofilaments, the additional factor $1/2$ for P_2 and P_3 takes into account that the appearance has to occur on the appropriate half of the proper one of the three visible protofilaments. Given the average rates λ_{app} and λ_{dis} shown in Table S1, and the total number of frames, we can estimate the expected number of occurrences, λ_1 , λ_2 , λ_3 , of the various events within the 441 recorded frames by multiplying P_1 , P_2 and P_3 with 418 and the average number of motors per frame (table S2).

Again assuming Poisson statistics, we can finally estimate the cumulative probabilities to obtain by chance the respective observed number or more of events of the three types in the random scenario, given the expected numbers of events:

$$CP_1(k \geq 29) = 1 - \sum_{k=0}^{28} \frac{(\lambda_1)^k e^{-\lambda_1}}{k!} \quad \text{Eq. S5}$$

$$CP_2(k \geq 8) = 1 - \sum_{k=0}^7 \frac{(\lambda_2)^k e^{-\lambda_2}}{k!} \quad \text{Eq. S6}$$

$$CP_3(k \geq 2) = 1 - \sum_{k=0}^1 \frac{(\lambda_3)^k e^{-\lambda_3}}{k!} \quad \text{Eq. S7}$$

Because we can, typically, only observe displacements up to ~ 90 nm, it is very unlikely to observe more than 3-step frame events with the frame rates we were using. Our statistical analysis results in upper limits of the probabilities for “false stepping events” and neglects some details of the experimental conditions, such as the frame acquisition time that varied from movie to movie. Still the very low probability values for false events strongly support our conclusion that most of the observed motility events indeed show single motors proceeding along protofilaments.

Table S2. Probability analysis. Expected numbers of 1-, 2-, 3-step “false” motility events λ_1 , λ_2 , λ_3 , (second column), actually observed events (third column) and the cumulative probabilities to obtain the respective number of observations, or more, from a Poissonian process of detachment/attachment with the given average rates (fourth column). For the numbers of observed events we also counted each 2-step event as two 1-step events, and each 3-step event as two 2-step and three 1-step events.

steps	expected events	observed events	probability
1	4.9	28	$1 \cdot 10^{-12}$
2	$1.2 \cdot 10^{-2}$	8	$1 \cdot 10^{-20}$
3	$3.1 \cdot 10^{-5}$	2	$5 \cdot 10^{-10}$